Science of the Total Environment 699 (2020) 134357

Contents lists available at ScienceDirect

Science of the Total Environment

journal homepage: www.elsevier.com/locate/scitotenv

Primary emissions and secondary organic aerosol formation from in-use diesel vehicle exhaust: Comparison between idling and cruise mode

Wei Deng [a], Zheng Fang [a,b], Zhaoyi Wang [a], Ming Zhu [a,b], Yanli Zhang [a,c], Mingjin Tang [a], Wei Song [a,c], Scott Lowther [a,d], Zhonghui Huang [e], Kevin Jones [d], Ping'an Peng [a], Xinming Wang [a,c,*]

[a] State Key Laboratory of Organic Geochemistry and Guangdong Key Laboratory of Environmental Protection and Resources Utilization, Guangzhou Institute of Geochemistry, Chinese Academy of Sciences, Guangzhou 510640, China
[b] University of Chinese Academy of Sciences, Beijing 100049, China
[c] Center for Excellence in Regional Atmospheric Environment, Institute of Urban Environment, Chinese Academy of Sciences, Xiamen 361021, China
[d] Lancaster Environment Centre, Lancaster University, Lancaster LA1 4YQ, United Kingdom
[e] South China Institute of Environmental Science, Ministry of Ecology and Environment, Guangzhou 510655, China

HIGHLIGHTS

- Diesel vehicle primary emissions and SOA formation were studied using smog chamber.
- Emission factors of AHs, PAHs and OVOCs deceased with the increasing driving speeds.
- Comparable BC and POA emissions but lower SOA productions at cruising than at idling;
- Eight OVOCs altogether could explain 8.4–23% SOA production.
- Total BC/POA/SOA at idling dropped 32% as fuel upgraded from China-3 to China-5.

GRAPHICAL ABSTRACT

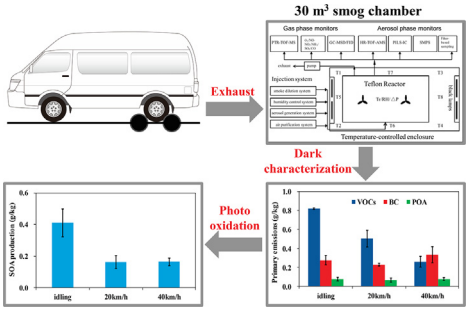

ARTICLE INFO

Article history:
Received 9 July 2019
Received in revised form 5 September 2019
Accepted 6 September 2019
Available online 7 September 2019

Editor: Jianmin Chen

ABSTRACT

Diesel vehicle exhaust is an important source of carbonaceous aerosols, especially in developing countries, like China. Driving condition impacts diesel vehicle emissions, yet its influence needs further understanding especially on secondary organic aerosol (SOA) formation. In this study tailpipe exhaust from an in-use light duty diesel vehicle at idling and driving speeds of 20 and 40 km h^{-1} was introduced respectively into a 30 m^{-3} indoor smog chamber to investigate primary emissions and SOA formation during photo-oxidation. The emission factors of SO_2 at 20 and 40 km h^{-1} were higher than those at idling, whereas the emission factors of aromatic hydrocarbons (AHs), polycyclic aromatic hydrocarbons (PAHs) and oxygenated volatile organic compounds (OVOCs) decreased when driving speeds increased. The emission factors of black carbon (BC) and primary organic aerosol (POA) at idling were comparable to those at 20 and 40 km h^{-1}. The SOA production factors were 0.41 ± 0.09 g kg-$fuel^{-1}$ at idling, approximately 2.5 times as high as those at 20 km h^{-1} (0.16 ± 0.09 g kg-$fuel^{-1}$) or 40 km h^{-1} (0.17 ± 0.09 g kg-$fuel^{-1}$). Total carbonaceous aerosols, including BC, POA and SOA, from diesel vehicles at 20 and 40 km h^{-1} were 60–75% of those at idling, due largely to a reduction in SOA production. Measured AHs and PAHs altogether were estimated to explain <10% of SOA production, and eight major OVOCs could contribute 8.4–23% of SOA production. A preliminary comparison was further made for the same diesel vehicle at idling using diesel oils upgraded from China 3 to China 5 standard. The emission factors of total particle

* Corresponding author at: State Key Laboratory of Organic Geochemistry, Guangzhou Institute of Geochemistry, Chinese Academy of Sciences, China.
E-mail address: wangxm@gig.ac.cn (X. Wang).

https://doi.org/10.1016/j.scitotenv.2019.134357

numbers decreased by 38% owing to less nuclei mode particles, which was probably caused by the reducing fuel sulfur content; the emission factors of BC were almost unchanged, the POA emission factors and SOA production factors however decreased by 72% and 37%.

1. Introduction

Motor vehicle exhaust is a major source of particulate matters with aerodynamic diameters <2.5 μm ($PM_{2.5}$) in urban areas (Jimenez et al., 2009; McDonald et al., 2015; Gentner et al., 2017), thus has significant effects on air quality and human health (Parrish and Zhu, 2009; Pope et al., 2009; Y. Wang et al., 2014; Lelieveld et al., 2015; Z. Liu et al., 2015). Diesel vehicle exhaust dominates the primary emission of PM from motor vehicles (Reff et al., 2009; Zhang et al., 2009), such like in China, in 2016 over 90% of PM emitted from mobile sources were attributed to diesel vehicles according to China vehicle environmental management annual report (MEPPRC, 2017). Numerous studies have been conducted to characterize primary emissions from diesel vehicles, including those using portable emission measurement systems (PEMS) or tunnel tests (Allen et al., 2001; Huang et al., 2006; Collins et al., 2007; Liu et al., 2009; Zhang et al., 2016; Cui et al., 2017), which could provide useful information about primary emissions from diesel vehicles under real-world traffic conditions. Driving condition is supposed to be an important factor influencing vehicle emission. Shah et al. (2004) found that emissions of PM, elemental carbon (EC) and organic carbon (OC) from a number of heavy duty diesel trucks under real-world conditions depended strongly on vehicle operation modes, with larger emission of EC and lower emission of OC found in the cruise mode compared to that of idling mode; in contrast, Chirico et al. (2010) found that for the same vehicle the emission factors of BC and POA at the driving speed of 60 km h^{-1} were comparable to those at idling. This inconsistency suggests that we have limited knowledge on how emissions might be effected by driving conditions, and highlights that the influence of driving conditions on primary emissions as well as secondary aerosol production needs further investigation.

Diesel exhaust also contributes substantially to secondary aerosols, particularly secondary organic aerosols (SOA), when photochemically oxidized and/or aged in ambient air (Gentner et al., 2012). Chamber simulation is an effective approach to investigate both primary emission and SOA formation from diluted exhausts of diesel engines or diesel vehicles (Robinson et al., 2007; Weitkamp et al., 2007; Chirico et al., 2010; Samy and Zielinska, 2010; Nakao et al., 2011; Gordon et al., 2014). Chamber studies in the USA and in Europe revealed organic aerosol (OA) enhancement ratios ranging from ~3 to 10 with the photochemical aging of diesel vehicle exhaust (Chirico et al., 2010; Gordon et al., 2014), while similar studies in China found an average enhancement ratio of 2.2 for exhausts from three in-used diesel vehicles (Deng et al., 2017). These studies, however, were mainly conducted at idling conditions, during which only 7% of total on-road diesel consumption were accounted for (Gaines et al., 2006). As the engine load is different between idling and driving conditions, primary emissions and SOA formation may also vary. Cross et al. (2015) found that the emission of intermediate volatile organic compounds (IVOCs) from diesel engines decreased rapidly when engine loads increased. Moreover, Miracolo et al. (2012) showed that SOA productions from diluted exhaust of gas-turbine engine at cruise modes were lower than those at idling modes. Therefore, the SOA formation from diesel vehicle exhausts at driving conditions might be different to that at idling conditions and deserved further investigation.

Tkacik et al. (2014) combined tunnel tests with a potential aerosol mass flow reactor to investigate the SOA formation from in-use vehicle emissions. While this approach provides SOA formation potential from actual traffic fleet exhausts under real-world driving condition, the effects of different factors (e.g., driving conditions, vehicle types, fuel quality, and etc.) on SOA formation cannot be assessed in a systematic manner. Combining chassis dynamometer tests together with chamber simulation makes it possible to obtain both the primary emissions and SOA production from a diesel vehicle at different driving condition. Using this approach, Chirico et al. (2010) investigated the primary emissions and SOA formation from medium duty diesel vehicle exhausts at idling and at a driving speed of 60 km h^{-1}, and concluded that the formed SOA at the driving speed of 60 km h^{-1} was comparable to that at idling. However, Gordon et al. (2014) compared the primary emissions and SOA production from a heavy duty diesel vehicle under idling and urban dynamometer driving schedule (UDDS) conditions, and suggested that the SOA production under the UDDS condition was much lower than that under the idling condition. Therefore, the effects of driving speeds on SOA formation from diesel vehicle exhausts also remains largely unknown, and further investigation is warranted.

According to China Vehicle Environmental Management Annual Report (MEPPRC, 2017), in China 94.6% diesel vehicles are not equipped with exhaust gas aftertreatment system, and 51.7% of them are China 3 diesel vehicles, which share a burden of 72.8% hydrocarbons and 68.6% particle matters emitted from diesel vehicles. In this study, a light duty diesel vehicle with China 3 emission standard was chosen and tested on a chassis dynamometer. The exhausts were diluted and introduced into an indoor smog chamber to measure primary emissions and to investigate SOA production with photo-oxidation. Thus we could obtain the emission factors of SO_2, volatile organic compounds (VOCs), BC and POA, as well as the SOA production factors from the diesel vehicles under idling, 20 and 40 km h^{-1}. This is follow-up work of our previous study (Deng et al., 2017), in which only the primary emissions and SOA formation from diesel vehicles at idling condition were investigated. The main purpose of this study is to investigate the influence of driving conditions on primary emissions and SOA formation from diesel vehicle exhausts. The results could enhance the understanding of both primary and secondary contribution of diesel vehicle exhausts to PM under real world condition.

2. Materials and methods

2.1. The diesel vehicle and fuels

An in-use passenger diesel vehicle made by Foton Motor was chosen in this study. Detailed information of this vehicle can be found in Table S1. In brief, it is a China 3 (identical to Euro 3) emission standard light duty diesel vehicle equipped with a four-cylinder, inline, direct-injection, turbocharged diesel engine. The same vehicle was chosen in our previous study (Deng et al., 2017), but its mileage had increased to 210,500 km from 160,000 km at the time of our previous study. It had no exhaust aftertreatment devices and was fueled with Grade 0# diesel purchased from a local gas station. It is worth noting that China 5 diesel fuel standard has been enforced in Guangdong since 2015, and

Table 1
Experimental conditions for the chamber experiments, as well as SOA formed during photo-oxidation.

Expt. no.	Speed ($km\ h^{-1}$)	T (°C)	RH (%)	NO[a] (ppbv)	NO_2[a] (ppbv)	Dilution ratio	OH exposure (10^7 molecules cm^{-3} h)	BC ($\mu g\ m^{-3}$)	POA ($\mu g\ m^{-3}$)	SOA[b] ($\mu g\ m^{-3}$)
1	0	25.0	5.6	474	54	263	2.5	20.3	4.9	28.5
2	0	24.4	2.7	318	61	376	0.6	14.5	4.6	26.9
3	0	24.9	5.8	625	58	252	2.2	31.4	8.5	38.4
4	20	25.6	3.8	1073	9	196	1.7	41.3	9.5	28.4
5	20	24.8	8.3	620	53	245	2.4	28.6	12.6	27.9
6	20	25.0	5.9	1299	40	149	1.1	51.1	17.2	24.1
7	40	23.2	10.3	1238	3	181	2.1	86.7	15.8	33.6
8	40	24.9	4.3	934	110	137	2.1	59.4	15.4	36.3
9	40	25.2	4.3	859	28	268	3.1	48.6	13.4	26.7

[a] Before adding HONO.
[b] Wall loss corrected SOA.

thus the fuel used in this study complies with the China 5 diesel fuel standard and the fuel sulfur content was regulated to be <10 ppm, whereas the fuel used by the same vehicle in our previous study (Deng et al., 2017) was China 3 diesel fuel in which sulfur content was limited to <350 ppm.

2.2. Experimental setup

All the experiments were carried out in a 30 m^3 indoor smog chamber at Guangzhou Institute of Geochemistry, Chinese Academy of Sciences, and details of the smog chamber can be found elsewhere (X. Wang et al., 2014; T. Liu et al., 2015; Deng et al., 2017). In brief, 135 black lamps (1.2 m long, 60 W Philips/10R BL, Royal Dutch Philips Electronics Ltd., the Netherlands) were used as the light source, providing a NO_2 photolysis rate of 0.25 min^{-1}. Temperature was maintained at 25 °C with an accuracy of ±1 °C, and the relative humidity (RH) was set to <5% (Table 1). Prior to each experiment, the Teflon chamber was flushed with dry purified air for at least 5 whole exchanges of the reactor volume to ensure that background concentrations of hydrocarbons, O_3, NOx, and aerosol particles in the chamber reactor were all below the detection limits.

The vehicle was tested at idling as well as at driving speeds of 20 and 40 $km\ h^{-1}$ on an electric chassis dynamometer (FCDM-100, Foshan Analytical Instrument Co., Ltd., China). The average driving speeds were 21.1 ± 1.4 and 41.3 ± 1.7 $km\ h^{-1}$, respectively. Three repeated experiments were performed for each driving condition. The results are presented as their means and standard deviations for the three repeated experiments. At the beginning of each experiment, the tested vehicle was firstly started and run on-road for ~30 min, then it was driven onto chassis dynamometer, and exhaust at hot idling or at driving at 20 and 40 $km\ h^{-1}$ was first diluted using a Dekati® ejector dilutor (DI-1000, Dekati Ltd., Finland) before introduced through a stainless steel transfer line into the chamber filled with purified air (Fig. S1). The stainless steel transfer line was heated to 100 °C during the experiments to reduce the loss of intermediate/semi-volatile organic compounds (I/SVOC). When the particle mass reached approximately 50 $\mu g\ m^{-3}$, which is comparable to the annual average value of $PM_{2.5}$ in Guangzhou in 2014 (Guangzhou Environmental Protection Bureau, 2015), exhaust injection was stopped. The injection time typically lasted 30–60 min.

Similar to previous studies (Chirico et al., 2010; Presto et al., 2014; Gordon et al., 2014; Deng et al., 2017), nitrous acid (HONO) was delivered into the chamber as a source of hydroxyl radicals (OH). Propene was also introduced into the chamber to adjust the VOC/NOx ratio to ~3 ppbC/ppb, a typical value for urban environments (Guo et al., 2013). In addition, 60 ppbv deuterated butanol (butanol-d9) was also injected into the chamber as a tracer for OH radicals, and the second-order rate constant for its reaction with OH radicals is 3.4×10^{-12} cm^3 $molecule^{-1}$ s^{-1} at room temperature (Barmet et al., 2012; Deng et al., 2017). After the primary emissions were characterized in the dark for 1 h, black lamps were turned on and the exhaust was photochemically aged for about 5 h. Although the particle mass and VOC/NOx ratio were similar to those in ambient air condition, the SOA formation from diesel vehicle exhausts simulated in the chamber might be different with that in ambient air due to different compositions between diesel and ambient PM as well as much higher levels of NOx and other pollutants in the chamber than in the ambient.

2.3. Instrumentation

An array of instruments was used to characterize gaseous and particulate species inside the chamber. Gas phase organic species were measured online with a commercial proton-transfer-reaction time-of-flight mass spectrometer (PTR-ToF-MS, Model 2000, Ionicon Analytik GmbH, Austria) operated in H_3O^+-ion mode (Lindinger et al., 1998; Jordan et al., 2009). The concentrations of hydroxyl radical (OH) during the experiments were inferred from the measured decay of deuterated butanol by the PTR-ToF-MS (Atkinson and Arey, 2003). The PTR-ToF-MS was calibrated weekly using a custom gas standard (Huang et al., 2016). Dedicated gas monitors were used to measure O_3 (EC9810, Ecotech, Australia), NOx (EC9841, Ecotech, Australia), and SO_2 (Model 43i, Thermo Scientific, USA). Before and after exhaust was introduced into the chamber, air samples were collected using 3 L cleaned Teflon bags to determine CO_2 concentrations using a HP 4890D gas chromatography (Yi et al., 2007). The dilution ratios were estimated by the measured CO_2 concentrations, and the results are shown in Table 1. Particle size distributions were measured with a scanning mobility particle sizer (SMPS, Model 3936, TSI Inc., Minnesota, USA), consisting of an electrostatic classifier (Model 3080), a long differential mobility analyzer (Model 308100), and a condensation particle counter (Model 3775). Particle mass concentrations were calculated by assuming that particles were spherical and had a density of 1.0 $g\ cm^{-3}$ (Weitkamp et al., 2007; Deng et al., 2017). BC concentrations were measured using a seven-wavelength Aethalometer (Model AE-31, Magee Scientific, Berkeley, California, USA), and the data were corrected for particle loading effects using the method of Kirchstetter and Novakov (2007). Mass concentrations and chemical compositions of submicron non-refractory aerosol particles were measured using a high-resolution time-of-flight aerosol mass spectrometer (HR-ToF-MS, Aerodyne Research Inc., USA) operated in alternating V and W modes (Jayne et al., 2000; DeCarlo et al., 2006). The mass concentration of particles measured by HR-ToF-AMS was corrected by SMPS data using the same method as Gordon et al. (2014) and T. Liu et al. (2015). The contribution of gas phase CO_2 to the AMS signals at m/z 44 was corrected

by analyzing HEPA filtered air from the smog chamber after it was filled with the exhaust.

2.4. Data analysis

The emission factors (EF) for various pollutants and the production factor (PF) for SOA were calculated on a fuel basis (g kg-fuel^{-1}) (Gordon et al., 2014) and presented in Table S2:

$$EForPF = 10^3 \cdot \frac{[\Delta P]}{[\Delta CO_2]} \cdot \frac{M(CO_2)}{M(C)} \cdot C_f \quad (1)$$

where $[\Delta P]$ and $[\Delta CO_2]$ are the background-corrected concentrations (μg m^{-3}) of the pollutants under investigation and CO_2, and $M(CO_2)$ and $M(C)$ are molar masses of CO_2 (44.1 g mol^{-1}) and C (12 g mol^{-1}), respectively. The mass fraction of carbon in the diesel fuel, C_f, is equal to 0.87 (Phuleria et al., 2006; Chirico et al., 2010). Similarly, the emission factor of total particle number (EF_{TN}, # kg-fuel^{-1}) was calculated using Eq. (2):

$$EF_{TN} = 10^{15} \cdot \frac{[PN_{tot}]}{[\Delta CO_2]} \cdot \frac{M(CO_2)}{M(C)} \cdot C_f \quad (2)$$

where $[PN_{tot}]$ is the total particle number concentration (# cm^{-3}).

The loss of particles and condensable organic vapors onto the reactor wall needs to be taken into account (Gordon et al., 2014). In this study, the AMS and SMPS data were corrected for wall loss using the method of Chirico et al. (2010). In brief, particulate loss was quantified by assuming that the aerosol was internally mixed and thus OA had the same wall loss rate as BC, and the mass concentration of OA corrected for wall losses (OA_{WLC}) can be estimated using Eq. (3):

$$OA_{WLC} = OA_{sus}(t) \times [BC(0)/BC(t)] \quad (3)$$

where $OA_{sus}(t)$ is the mass concentration of suspended OA measured using HR-ToF-AMS at the time of t, and BC(0) and BC(t) are the measured BC concentrations when the lamps were switched on and at the time of t, respectively. This correction is the $\omega = 1$ case in Gordon et al. (2014), where ω is a proportionality factor of organic vapor partitioning to chamber walls and suspended particles (Weitkamp et al., 2007). This means that organic vapors are in dynamic equilibrium with both wall-bound and suspended particles. Previous studies suggested that organic vapors not only can lose to wall-bound particles, but also can lose directly to the chamber wall, the directly loss of organic vapor to the chamber walls could lead to an underestimation of the SOA formation potential (Yeh and Ziemann, 2014; Zhang et al., 2014, 2015; Ye et al., 2016). To evaluate the performance of our wall loss correction method in accounting for the vapor wall loss, the vapor loss directly to chamber walls was also estimated by assigning a condensational sink to the chamber walls. Details can be found in the supporting information. As shown in Fig. S2, our approach of determining SOA formation could account for vapor wall loss as Zhao et al. (2017) in gasoline exhaust experiments. Moreover, the CS of suspended particles was 0.174 ± 0.020, 0.206 ± 0.081, and 0.346 ± 0.174 min^{-1} for idling, 20 and 40 km h^{-1}. The similarity in CS of suspended particles in different experiments indicates that the changes in SOA formation were not due to the biases caused by the vapor wall loss.

3. Results and discussion

3.1. Primary emissions

3.1.1. Gaseous pollutants

Fig. 1 displays the emission factors of aromatic hydrocarbons (AHs), polycyclic aromatic hydrocarbons (PAHs) and eight oxygenated volatile organic compounds (OVOCs), including furan, methacrolein, methylfuran, phenol, dimethylfuran, cresol, benzenediol and dimethylphenol, measured by the PTR-ToF-MS. The emission factors of those organic species decreased with increasing of driving speeds, detailed data is listed in Table S2. Benzene and toluene dominated the emission of AHs, and their emission factors were measured to be 0.21 ± 0.01 and 0.12 ± 0.03 g kg-fuel^{-1} for idling, 0.09 ± 0.01 and 0.04 ± 0.01 g kg-fuel^{-1} for 20 km h^{-1}, and 0.04 ± 0.01 and 0.02 ± 0.01 g kg-fuel^{-1} for 40 km h^{-1}. The contributions of other AHs were minor. The emission factors of $C_{10}H_8$ (naphthalene), $C_{12}H_8$ (acenaphthylene) and $C_{12}H_{10}$ (acenaphthene) were 4.75 ± 1.17, 5.13 ± 1.22 and 1.68 ± 0.21 mg kg-fuel^{-1} for idling, 3.31 ± 0.90, 3.32 ± 0.37 and 1.50 ± 0.62 mg kg-fuel^{-1} for 20 km h^{-1}, and 2.38 ± 1.41, 1.30 ± 0.23 and 0.49 ± 0.17 mg kg-fuel^{-1} for 40 km h^{-1}.

As shown in Fig. 2, the emission factor of SO_2 at idling in this study was 0.05 ± 0.01 g kg-fuel^{-1}, which was comparable to that (0.06 ± 0.03 g kg-fuel^{-1}) for a Euro 3 diesel vehicle fueled by ultra-low sulfur diesel with a fuel sulfur content <15 ppm (Zavala et al., 2017). The emission factors of SO_2 for 20 and 40 km h^{-1} (0.07 ± 0.02 and 0.07 ± 0.01 g kg-fuel^{-1}), which were a little bit higher than those at idling condition. Assuming that all SO_2 emission came from diesel burning and all sulfur in the diesel was converted to SO_2, the diesel sulfur contents were estimated to be 26–

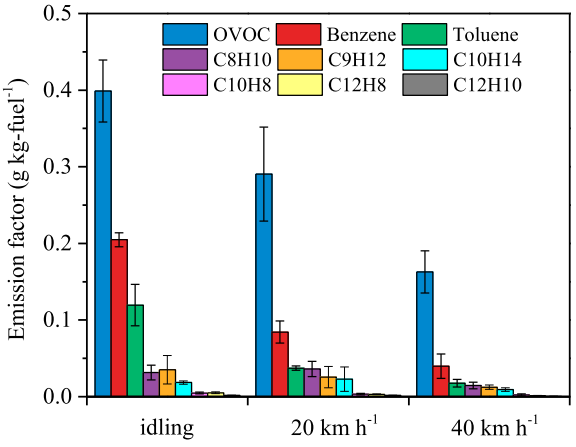

Fig. 1. Emission factors of OVOCs, AHs and PAHs in gas phase as measured using PTR-ToF-MS for idling, 20 and 40 km h^{-1}.

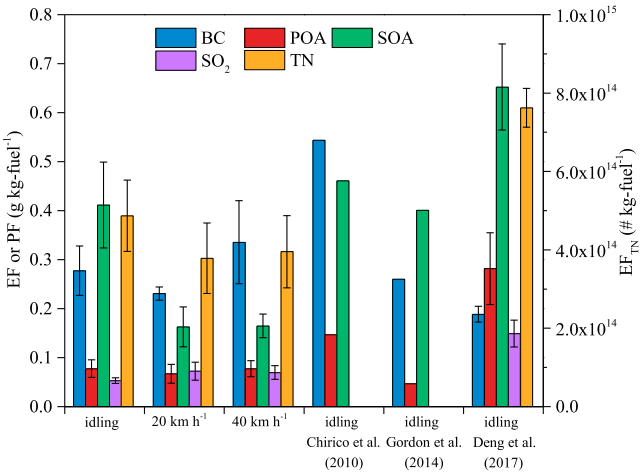

Fig. 2. Emission factors of BC (left y-axis), POA (left y-axis), SO_2 (left y-axis), total particle number (right y-axis), and production factors of SOA (left y-axis): comparison of our results (idling, 20 and 40 km h^{-1}) with previous studies (idling).

35 ppm, higher than the limit of 10 ppm in China 5 diesel, suggesting that the sulfur content of diesel used in this study was beyond the limit, or other sources might also contributed to SO_2 emission.

3.1.2. Particulate matters

Fig. 2 shows emission factors of BC, POA, and total particle number measured in this study in comparison with those in previous studies for idling diesel vehicles without aftertreatment devices. The average emission factors of BC were 0.28 ± 0.05, 0.23 ± 0.01 and 0.34 ± 0.09 g kg-fuel^{-1}, and that of POA were 0.08 ± 0.02, 0.07 ± 0.02 and 0.08 ± 0.02 g kg-fuel^{-1}, respectively, for idling, 20 and 40 km h^{-1}. At idling condition, the emission factors of BC and POA measured in our work were consistent with those of 0.260 and 0.047 g kg-fuel^{-1} reported by Gordon et al. (2014), but lower than those of 0.544 and 0.147 g kg-fuel^{-1} reported by Chirico et al. (2010). The emission factors of total particle number (PN) for idling, 20 and 40 km h^{-1} were measured to be 4.64 ± 1.12 × 10^{14}, 3.78 ± 0.90 × 10^{14} and 3.95 ± 0.92 × 10^{14} kg-fuel^{-1}, respectively. Our results were within the range of 0.3–21 × 10^{14} kg-fuel^{-1} reported for city buses under real-world conditions in Finland (Pirjola et al., 2016). Assuming an average diesel efficiency of 8.6 L per 100 km and a diesel oil density of 0.85 g mL^{-1} (Table S1; Zhang et al., 2016), the mileage-based emission factors of PN for the vehicle tested in our work were in the range of 2.22–4.31 × 10^{13} km^{-1}, much higher than the EU limit of 6.0 × 10^{11} km^{-1} (EU commission regulation No. 459/2012, 2012).

Our work demonstrated that the diesel vehicle had emission factors of both BC and POA at 20 or 40 km h^{-1} comparable to those at idling. This result is consistent with Chirico et al. (2010) where emission factors of BC and POA at 60 km h^{-1} were comparable to those at idling. However, Shah et al. (2004) found larger emission of EC in the cruise mode than in the idling mode, and lower emission of OC in the cruise mode than in the idling mode. Our work and the work by Chirico et al. (2010) were both conducted on a chassis dynamometer with relatively steady engine loads under constant driving speeds; In contrast, on-road tests were performed by Shah et al. (2004) and the engine loads could vary when driving uphill, downhill, and on flat road even the driving speed was kept steady. Nevertheless, based on on-road tests using PEMS for 25 heavy duty diesel vehicles (Zheng et al., 2015), BC emissions became stable when the average speeds ranged from 30 km h^{-1} to 70 km h^{-1}. Therefore, more works are necessary about the influence of driving speeds and engine loads on primary emissions.

3.2. SOA formation

After the diesel vehicle exhaust was photochemically aged for 5 h in the indoor chamber, significant amounts of SOA were formed. As shown in Fig. 2, the SOA production factors were found to be 0.41 ± 0.09 g kg-fuel^{-1} at idling, similar to that of 0.461 kg-fuel^{-1} reported by Chirico et al. (2010) or 0.401 kg-fuel^{-1} reported by Gordon et al. (2014) for idling diesel vehicles without aftertreatment. The SOA/POA ratios were found to range from 4.5 to 5.9, higher than that of ~3 reported by Chirico et al. (2010) for a medium duty diesel vehicle at idling, but significantly smaller than that of ~10 reported by Gordon et al. (2014) for a heavy duty diesel vehicle in the US under the "creep + idle" condition.

The SOA production factors were measured to be 0.16 ± 0.04 g kg-fuel^{-1} at 20 km h^{-1}and 0.17 ± 0.02 g kg-fuel^{-1} at 40 km h^{-1}, being only ~30% of that for the idling condition. The SOA/POA ratios were 2.0 to 3.1, lower than those under idling condition. This is consistent with Jathar et al. (2017) where SOA formation at load condition was higher than that at idling. Zhao et al. (2015) found that the averaged ratio of the total IVOCs to POA was 20.4 ± 3.7 for the "creep + idle" condition and it decreased to 8.0 ± 3.6 for the driving condition. Since our study showed that the POA emission factors were near each other for idling or for driving at 20/40 km h^{-1}, if the ratio of the total IVOCs to POA changed the same as reported by Zhao et al. (2015), the emission factors of total IVOCs for idling would be ~2.5 times as high as those for driving at 20 and 40 km h^{-1}. As discussed above, the emission factors of the PAHs, which are IVOC species, decreased with the increase of driving speed (Fig. 1). Zhao et al. (2015) suggested that IVOCs could dominate the SOA production for diesel vehicle exhaust. Hence, the larger SOA production factors at idling might be at least partly attributed to larger IVOC emissions.

Combining BC, POA and SOA altogether, the contributions of diesel vehicle exhaust to carbonaceous aerosols at 20 and 40 km h^{-1} were 60–75% of those at idling condition, and the reduction was mainly caused by the lower SOA production. This also implies mitigating traffic congestion to reduce idling conditions would be an effective way to lower diesel vehicles' overall contribution to fine particles in urban areas.

3.3. Contribution of different precursors to SOA formation

SOA productions from traditional precursor VOCs ($SOA_{predicted}$) measured by PTR-ToF-MS can be estimated using Eq. (4):

$$SOA_{predicted} = \sum_i \Delta X_i \times Y_i \quad (4)$$

where ΔX_i is the mass concentration (μg m^{-3}) of the ith precursor consumed during photochemical oxidation, and Y_i is the corresponding SOA yield of ith precursor. As the PTR-ToF-MS cannot distinguish isomers, AHs were divided into five groups, including benzene, toluene, C2-benzene, C3-benzene, and C4-benzene. The SOA yields for benzene, toluene and m-xylene were estimated using the two-product model (Ng et al., 2007), and styrene was assumed to have the same SOA yield as m-xylene. The SOA yields for C3-benzene and C4-benzene were taken from Odum et al. (1997).

Fig. 3 displays the predicted relative contributions of different groups of precursor VOCs to the total measured SOA for idling, 20 km h^{-1} and 40 km h^{-1}. Although the emission factors of AHs were different at idling, 20 and 40 km h^{-1}, the contribution percentages to SOA formation were similar and minor, and they were 3.2 ± 0.5%, 4.3 ± 1.0% and 2.6 ± 0.8%, respectively. Weitkamp et al. (2007) reported that <10% of the SOA mass can be explained by the known precursors for diesel exhaust experiments; Deng et al. (2017) noticed that 65 non-methane hydrocarbons accounted for <3% of the SOA production from diesel exhausts. Previous studies found that naphthalene can contribute as much as 52% of gasoline SOA (T. Liu et al., 2015) and approximate 16% of SOA from wood combustion plumes (Bruns et al., 2016). The SOA formation from three PAHs, including naphthalene, acenaphthylene and acenaph-

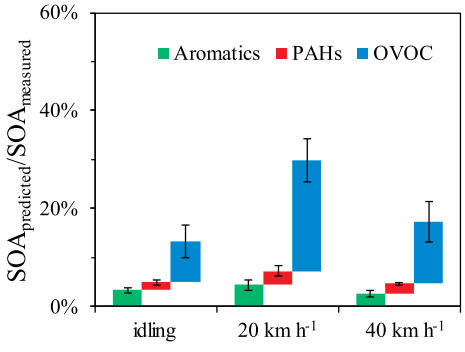

Fig. 3. Predicted relative contributions of AHs, PAHs and OVOCs to the total formed SOA for experiments in which the diesel vehicle was operated in different modes.

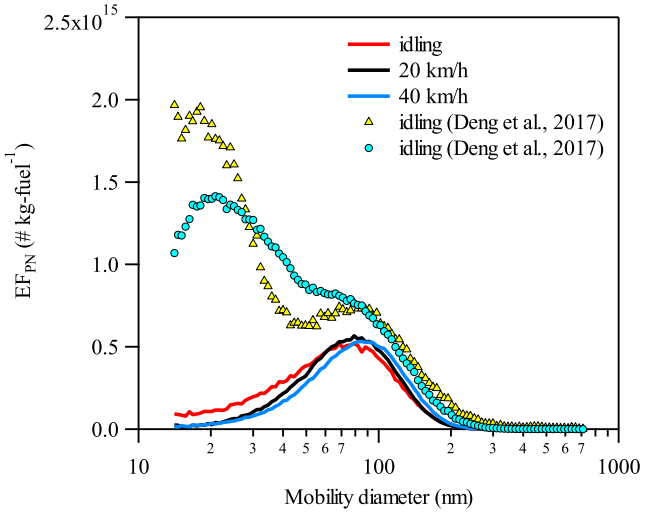

Fig. 4. Number distributions of the particles from Foton light duty diesel vehicle exhaust with China 5 diesel under idling, 20 and 40 km h^{-1} (lines), as well as the particle number distribution for Foton light duty diesel vehicle with China 3 diesel under idling condition (markers). The vertical axis was converted to emission factors of particle number (EF_{PN}) with Eq. (2).

thene, were estimated. According to the gas-particle partition theory, over 98% of these three PAHs were in gas phase, and the data from HR-ToF-AMS confirmed that (Table S3). Therefore, the SOA contribution from particle phase naphthalene, acenaphthylene and acenaphthene was minor compared to that from their gas phase. With the SOA yields reported by Shakya and Griffin (2010), the contribution of three PAHs to the measured SOA was estimated to be only 1.6–2.9% in all experiments. The measured AHs and PAHs altogether were estimated to account for <10% of SOA production.

Previous studies suggested that OVOCs, such as phenol, benzenediol, and cresol, were very important SOA precursors in biomass burning plumes (Bruns et al., 2016; Fang et al., 2017). In this study, eight OVOCs were measured by the PTR-ToF-MS. The SOA production from these eight OVOCs was estimated by Eq. (4). The SOA yields depend on experimental conditions, including VOC/NOx ratios, presence of seed particles and total organic mass (Odum et al., 1997; Ng et al., 2007; Zhang et al., 2014). As the VOC/NOx ratios in this study (~3 ppbC/ppb) were much lower than the minimum ratio reported in the literature, the yields reported at the minimum VOC/NOx ratio was applied to estimate the SOA production (Table S4). The SOA production from the OVOCs was calculated to be 2.77 ± 1.51, 5.98 ± 0.74, and 3.95 ± 0.93 μg m^{-3} for idling, 20 and 40 km h^{-1}, and they accounted for 8.4 ± 3.4%, 23 ± 4.3%, and 13 ± 4.2% of the SOA formation from the diesel exhausts (Fig. 3), respectively. In summary, the total contribution percentages of detected AHs, PAHs and OVOCs to the formed SOA added up to 13–30%, suggesting that precursors other than these species might contribute substantially to SOA formation from diesel exhausts. It is worth noting that only eight OVOCs were considered in this study, the contribution of OVOCs to SOA formation from diesel exhausts could be even larger if more carbonyl compounds were taken into account, as carbonyls were the most abundant VOCs in diesel exhausts (Schauer et al., 1999; Yao et al., 2015).

3.4. Effect of fuel upgrade

The vehicle used in this study is the same one used in a previous study by Deng et al. (2017), yet its mileage increased about 55,000 km at the time of present study, and the diesel fuel it used had upgraded from grade China 3 to grade China 5. The BC emission factors measured in the present work were quite similar with that in our previous study (Deng et al., 2017). The emission factors of POA and the total PN, however, decreased by 72% and 38%, respectively. Fig. 4 displayed the number distributions of particles emitted by the diesel vehicle. While only one peak with a median diameter of 80 nm, which was probably related to soot particles (Rönkkö et al., 2007, 2013), was observed at idling, 20 and 40 km h^{-1} in this study. The peak of nuclei mode particles with a median diameter of 10 nm were not observed in this work but significant amount of nuclei mode particles appeared in our previous study (Deng et al., 2017). Therefore the decrease in total PN emission was mainly due to less nuclei mode particles.

It has been suggested that the emission of nuclei mode particles increases with the increase in the fuel sulfur content, while the emission of soot mode particles is not affected (Sakurai et al., 2003; Liu et al., 2007; Rönkkö et al., 2013). The diesel fuel used in this study was China 5 grade with a sulfur content limit of 10 ppm (Table S4), and that in the study by Deng et al. (2017) was China 3 grade with a sulfur content limit of 350 ppm. As shown is Fig. 1, the average SO_2 emission factor was 0.05 g kg-$fuel^{-1}$ for idling in this study, 36% of that (0.15 g kg-$fuel^{-1}$) measured in our previous study (Deng et al., 2017). Assuming that SO_2 all came from the conversion of sulfur in the diesel fuel, the fuel sulfur contents were estimated to be 25 ppm in this study and 75 ppm in Deng et al. (2017). Therefore, the difference in the fuel sulfur content might be the reason that causes the differences in total PN and their size distribution between this study and our previous study (Sakurai et al., 2003; Liu et al., 2007; Rönkkö et al., 2013).

Compared with our previous study (Deng et al., 2017) with the same diesel vehicle at idling, the SOA production factors measured in this work decrease by 37%. The CS of suspended particles in this study (0.174 ± 0.020 min^{-1}) was similar to that (0.154 ± 0.060 min^{-1}) in Deng et al. (2017), indicating that the reduction in SOA formation was not due to the biases caused by organic vapor wall loss. The temperature was 24.8 ± 0.5 °C, RH was <6% (Table 1), and VOC/NOx ratios were ~3 ppbC/ppb both in this study and in Deng et al. (2017), also indicating that the decrease was not due to the biases caused by the change of experimental conditions. As shown in Fig. S4, the van Krevelen slopes in this study were also similar to those in Deng et al. (2017), indicating the SOA precursors and formation pathways might also be similar. Both studies revealed that the measured traditional precursor VOCs could only account for <10% of SOA observed and IVOCs might dominate the SOA production; if the IVOC/POA ratios were the same, the IVOCs emission in this study should be lower due to lowered POA emissions. Unfortunately, IVOCs were not measured in the two studies, and identification and quantification of IVOCs (as well as their SOA production yields) should be further investigated for a better understanding of the SOA formation from diesel vehicle exhaust.

In summary, the total mass concentrations of BC, POA and SOA from diesel vehicle decreased approximately by 32% due to the upgrading of diesel fuel from China 3 to China 5. It is worth noting that as the vehicle's mileage accumulated from 160,000 km to 210,500 km, primary emissions and thereby SOA formation are supposed to increase due to the deterioration of engine if there is no fuel switch (Clark et al., 2002; Maricq et al., 2013). Therefore, the reduction of primary emissions and SOA formation due to fuel switch might be underestimated if considering the mileage accumulation and engine deterioration. Our work demonstrated that upgrading diesel fuel could help lower the emission of POA and the total PN and reduce SOA formation from diesel exhaust, but have no significant effects on BC emission. To further reduce BC emission, upgrade of engine technology and adoption of aftertreat-

ment devices, such as diesel particulate filters, are required (Chirico et al., 2010; Gordon et al., 2014).

4. Conclusions

In this study, we characterized primary emissions of gaseous species and particulate matters from an in-use China 3 light duty diesel vehicle at idling as well as driving at constant speeds of 20 and 40 km h^{-1}, and investigated their SOA formation when photochemically oxidized in a large indoor chamber. Emission factors of AHs, PAHs and OVOCs all decreased with the increase in driving speed. The emission factors of BC, POA and the total PN at driving speeds of 20/40 km h^{-1} were however comparable to those at idling.

After photochemical aging, significant amount of SOA was formed with SOA/POA ratios ranging from 2.0 to 5.9. The SOA production factors at 20 and 40 km h^{-1} were lower than those at idling. The total contribution of AHs, naphthalene, acenaphthylene, and acenaphthene to the formed SOA were estimated to be <10% of the observed SOA for all the driving conditions. OVOCs accounted for 8.4–23% of measured SOA production. At 20/40 km h^{-1} the combined contributions of BC, POA and SOA to carbonaceous aerosols were 60–75% of those at idling condition, largely due to reduced SOA production. This might be probably explained by the reduced emission of IVOCs as important precursors in diesel vehicle exhaust (Zhao et al., 2015). It should be emphasized that emission factors of IVOCs by diesel vehicles in China might be very different from those in the USA. Therefore, comprehensive characterization of IVOCs emitted by diesel vehicles in China are required to better understand the impacts of diesel vehicle emissions on air quality particularly in urban areas. In this study, only tests for constant driving speeds of 20 and 40 km h^{-1} were performed, more tests for driving cycles, which include acceleration and deceleration, should be conducted in the future in order to better reflect real world driving conditions.

Compared with our previous study (Deng et al., 2017) with the same diesel vehicle, the BC emission factors remained almost unchanged after a fuel switch from China 3 to China 5, while the POA emission factors and SOA production factors became significantly lower, and the emission factors of total particle numbers also decreased with reduced nuclei mode particles due probably to the reduction of fuel sulfur content. These results, however, are based on tests for only one diesel vehicle in this study. Tests involving with more diesel vehicles and under various driving conditions might be needed to deepen our understanding and to obtain more representative results.

Declaration of Competing Interest

The authors declare that they have no known competing financial interests or personal relationships that could have appeared to influence the work reported in this paper.

Acknowledgments

This study was supported by the National Key Research and Development Program (2016YFC0202204), the Strategic Priority Research Program of the Chinese Academy of Sciences (grant no. XDB05010200), the National Natural Science Foundation of China (grant no. 41530641/41571130031/41673116/41503105) and the Guangzhou Science, Technology and Innovation Commission (201607020002). The efforts of the two anonymous reviewers have greatly improved the quality of this manuscript and are sincerely appreciated.

Appendix A. Supplementary data

Supplementary data to this article can be found online at https://doi.org/10.1016/j.scitotenv.2019.134357.

References

Allen, J.O., Mayo, P.R., Hughes, L.S., Salmon, L.G., Cass, G.R., 2001. Emissions of size-segregated aerosols from on-road vehicles in the Caldecott tunnel. Environ. Sci. Technol. 35, 4189–4197. https://doi.org/10.1021/es0015545.

Atkinson, R., Arey, J., 2003. Atmospheric degradation of volatile organic compounds. Chem. Rev. 103, 4605–4638. https://doi.org/10.1021/cr0206420.

Barmet, P., Dommen, J., DeCarlo, P.F., Tritscher, T., Praplan, A.P., Platt, S.M., Prevot, A. S.H., Donahue, N.M., Baltensperger, U., 2012. OH clock determination by proton transfer reaction mass spectrometry at an environmental chamber. Atmos. Meas. Tech. 5, 647–656. https://doi.org/10.5194/amt-5-647-2012.

Bruns, E.A., El Haddad, I., Slowik, J.G., Kilic, D., Klein, F., Baltensperger, U., Prévôt, A.S. H., 2016. Identification of significant precursor gases of secondary organic aerosols from residential wood combustion. Sci. Rep. UK 6, 27881. https://doi.org/10.1038/srep27881.

Chirico, R., DeCarlo, P.F., Heringa, M.F., Tritscher, T., Richter, R., Prevot, A.S.H., Dommen, J., Weingartner, E., Wehrle, G., Gysel, M., Laborde, M., Baltensperger, U., 2010. Impact of aftertreatment devices on primary emissions and secondary organic aerosol formation potential from in-use diesel vehicles: results from smog chamber experiments. Atmos. Chem. Phys. 10, 11545–11563. https://doi.org/10.5194/acp-10-11545-2010.

Clark, N.N., Kern, J.M., Atkinson, C.M., Nine, R.D., 2002. Factors affecting heavy-duty diesel vehicle emissions. J. Air Waste Manage. Assoc. 52, 84–94. https://doi.org/10.1080/10473289.2002.10470755.

Collins, J.F., Shepherd, P., Durbin, T.D., Lents, J., Norbeck, J., Barth, M., 2007. Measurements of in-use emissions from modern vehicles using an on-board measurement system. Environ. Sci. Technol. 41, 6554–6561. https://doi.org/10.1021/es0627850.

Cross, E.S., Sappok, A.G., Wong, V.W., Kroll, J.H., 2015. Load-dependent emission factors and chemical characteristics of IVOCs from a medium-duty diesel engine. Environ Sci Technol 49, 13483–13491. https://doi.org/10.1021/acs.est.5b03954.

Cui, M., Chen, Y., Feng, Y., Li, C., Zheng, J., Tian, C., Yan, C., Zheng, M., 2017. Measurement of PM and its chemical composition in real-world emissions from non-road and on-road diesel vehicles. Atmos. Chem. Phys. 17, 6779–6795. https://doi.org/10.5194/acp-17-6779-2017.

DeCarlo, P.F., Kimmel, J.R., Trimborn, A., Northway, M.J., Jayne, J.T., Aiken, A.C., Gonin, M., Fuhrer, K., Horvath, T., Docherty, K.S., Worsnop, D.R., Jimenez, J.L., 2006. Field-deployable, high-resolution, time-of-flight aerosol mass spectrometer. Anal. Chem. 78, 8281–8289. https://doi.org/10.1021/ac061249n.

Deng, W., Hu, Q., Liu, T., Wang, X., Zhang, Y., Song, W., Sun, Y., Bi, X., Yu, J., Yang, W., Huang, X., Zhang, Z., Huang, Z., He, Q., Mellouki, A., George, C., 2017. Primary particulate emissions and secondary organic aerosol (SOA) formation from idling diesel vehicle exhaust in China. Sci. Total Environ. 593–594, 462–469. https://doi.org/10.1016/j.scitotenv.2017.03.088.

EU Commission Regulation No 459/2012. Commission Regulation (EU) No 459/2012 of 29 May 2012, 2012. Amending regulation (EC) no 715/2007 of the European Parliament and of the Council and Commission Regulation (EC) No 692/2008 as regards emissions from light passenger and commercial vehicles (Euro 6). Off. J. Eur. Union L 142, 16–24.

Fang, Z., Deng, W., Zhang, Y., Ding, X., Tang, M., Liu, T., Hu, Q., Zhu, M., Wang, Z., Yang, W., Huang, Z., Song, W., Bi, X., Chen, J., Sun, Y., George, C., Wang, X., 2017. Open burning of rice, corn and wheat straws: primary emissions, photochemical aging, and secondary organic aerosol formation. Atmos. Chem. Phys. 17, 14821–14839. https://doi.org/10.5194/acp-17-14821-2017.

Gaines, L., Vyas, A., Anderson, J.L., 2006. Estimation of fuel use by idling commercial trucks. Transport Res. Rec. 1983, 91–98. https://doi.org/10.3141/1983-13.

Gentner, D.R., Isaacman, G., Worton, D.R., Chan, A.W.H., Dallmann, T.R., Davis, L., Liu, S., Day, D.A., Russell, L.M., Wilson, K.R., Weber, R., Guha, A., Harley, R.A., Goldstein, A.H., 2012. Elucidating secondary organic aerosol from diesel and gasoline vehicles through detailed characterization of organic carbon emissions. Proc. Natl. Acad. Sci. U. S. A. 109, 18318–18323. https://doi.org/10.1073/pnas.1212272109.

Gentner, D.R., Jathar, S.H., Gordon, T.D., Bahreini, R., Day, D.A., El Haddad, I., Hayes, P. L., Pieber, S.M., Platt, S.M., de Gouw, J., Goldstein, A.H., Harley, R.A., Jimenez, J.L., Prevot, A.S., Robinson, A.L., 2017. Review of urban secondary organic aerosol formation from gasoline and diesel motor vehicle emissions. Environ Sci Technol 51, 1074–1093. https://doi.org/10.1021/acs.est.6b04509.

Gordon, T.D., Presto, A.A., Nguyen, N.T., Robertson, W.H., Na, K., Sahay, K.N., Zhang, M., Maddox, C., Rieger, P., Chattopadhyay, S., Maldonado, H., Maricq, M.M., Robinson, A.L., 2014. Secondary organic aerosol production from diesel vehicle exhaust: impact of aftertreatment, fuel chemistry and driving cycle. Atmos. Chem. Phys. 14, 4643–4659. https://doi.org/10.5194/acp-14-4643-2014.

Guangzhou Environmental Protection Bureau, 2015 „ Report on the State of the Environment in Guangzhou. ..

Guo, H., Ling, Z.H., Cheung, K., Jiang, F., Wang, D.W., Simpson, I.J., Barletta, B., Meinardi, S., Wang, T.J., Wang, X.M., Saunders, S.M., Blake, D.R., 2013. Characterization of photochemical pollution at different elevations in

mountainous areas in Hong Kong. Atmos. Chem. Phys. 13, 3881–3898. https://doi.org/10.5194/acp-13-3881-2013.
Huang, X.F., Yu, J.Z., He, L.Y., Hu, M., 2006. Size distribution characteristics of elemental carbon emitted from Chinese vehicles: results of a tunnel study and atmospheric implications. Environ. Sci. Technol. 40, 5355–5360. https://doi.org/10.1021/es0607281.
Huang, Z., Zhang, Y., Yan, Q., Zhang, Z., Wang, X., 2016. Real-time monitoring of respiratory absorption factors of volatile organic compounds in ambient air by proton transfer reaction time-of-flight mass spectrometry. J. Hazard. Mater. 320, 547–555. https://doi.org/10.1016/j.jhazmat.2016.08.064.
Jathar, S.H., Friedman, B., Galang, A.A., Link, M.F., Brophy, P., Volckens, J., Eluri, S., Farmer, D.K., 2017. Linking load, fuel, and emission controls to photochemical production of secondary organic aerosol from a diesel engine. Environ. Sci. Technol. 51, 1377–1386. https://doi.org/10.1021/acs.est.6b04602.
Jayne, J.T., Leard, D.C., Zhang, X., Davidovits, P., Smith, K.A., Kolb, C.E., Worsnop, D.R., 2000. Development of an aerosol mass spectrometer for size and composition analysis of submicron particles. Aerosol Sci. Technol. 33, 49–70. https://doi.org/10.1080/027868200410840.
Jimenez, J.L., Canagaratna, M.R., Donahue, N.M., Prevot, A.S., Zhang, Q., Kroll, J.H., DeCarlo, P.F., Allan, J.D., Coe, H., Ng, N.L., Aiken, A.C., Docherty, K.S., Ulbrich, I.M., Grieshop, A.P., Robinson, A.L., Duplissy, J., Smith, J.D., Wilson, K.R., Lanz, V.A., Hueglin, C., Sun, Y.L., Tian, J., Laaksonen, A., Raatikainen, T., Rautiainen, J., Vaattovaara, P., Ehn, M., Kulmala, M., Tomlinson, J.M., Collins, D.R., Cubison, M.J., Dunlea, E.J., Huffman, J.A., Onasch, T.B., Alfarra, M.R., Williams, P.I., Bower, K., Kondo, Y., Schneider, J., Drewnick, F., Borrmann, S., Weimer, S., Demerjian, K., Salcedo, D., Cottrell, L., Griffin, R., Takami, A., Miyoshi, T., Hatakeyama, S., Shimono, A., Sun, J.Y., Zhang, Y.M., Dzepina, K., Kimmel, J.R., Sueper, D., Jayne, J. T., Herndon, S.C., Trimborn, A.M., Williams, L.R., Wood, E.C., Middlebrook, A.M., Kolb, C.E., Baltensperger, U., Worsnop, D.R., 2009. Evolution of organic aerosols in the atmosphere. Science 326, 1525–1529. https://doi.org/10.1126/science.1180353.
Jordan, A., Haidacher, S., Hanel, G., Hartungen, E., Märk, L., Seehauser, H., Schottkowsky, R., Sulzer, P., Märk, T.D., 2009. A high resolution and high sensitivity proton-transfer-reaction time-of-flight mass spectrometer (PTR-TOF-MS). Int. J. Mass Spectrom. 286, 122–128. https://doi.org/10.1016/j.ijms.2009.07.005.
Kirchstetter, T.W., Novakov, T., 2007. Controlled generation of black carbon particles from a diffusion flame and applications in evaluating black carbon measurement methods. Atmos. Environ. 41, 1874–1888. https://doi.org/10.1016/j.atmosenv.2006.10.067.
Lelieveld, J., Evans, J.S., Fnais, M., Giannadaki, D., Pozzer, A., 2015. The contribution of outdoor air pollution sources to premature mortality on a global scale. Nature 525, 367–371. https://doi.org/10.1038/nature15371.
Lindinger, W., Hansel, A., Jordan, A., 1998. On-line monitoring of volatile organic compounds at pptv levels by means of proton-transfer-reaction mass spectrometry (PTR-MS) medical applications, food control and environmental research. Int. J. Mass Spectrom. Ion Process. 173, 191–241. https://doi.org/10.1016/S0168-1176(97)00281-4.
Liu, Z.G., Vasys, V.N., Kittelson, D.B., 2007. Nuclei-mode particulate emissions and their response to fuel sulfur content and primary dilution during transient operations of old and modern diesel engines. Environ. Sci. Technol. 41, 6479–6483. https://doi.org/10.1021/es0629007.
Liu, H., He, K., Lents, J.M., Wang, Q., Tolvett, S., 2009. Characteristics of diesel truck emission in China based on portable emissions measurement systems. Environ. Sci. Technol. 43, 9507–9511. https://doi.org/10.1021/es902044x.
Liu, T., Wang, X., Deng, W., Hu, Q., Ding, X., Zhang, Y., He, Q., Zhang, Z., Lü, S., Bi, X., Chen, J., Yu, J., 2015a. Secondary organic aerosol formation from photochemical aging of light-duty gasoline vehicle exhausts in a smog chamber. Atmos. Chem. Phys. 15, 9049–9062. https://doi.org/10.5194/acp-15-9049-2015.
Liu, Z., Guan, D., Wei, W., Davis, S.J., Ciais, P., Bai, J., Peng, S., Zhang, Q., Hubacek, K., Marland, G., Andres, R.J., Crawford-Brown, D., Lin, J., Zhao, H., Hong, C., Boden, T. A., Feng, K., Peters, G.P., Xi, F., Liu, J., Li, Y., Zhao, Y., Zeng, N., He, K., 2015b. Reduced carbon emission estimates from fossil fuel combustion and cement production in China. Nature 524, 335–338. https://doi.org/10.1038/nature14677.
Maricq, M.M., Szente, J.J., Adams, J., Tennison, P., Rumpsa, T., 2013. Influence of mileage accumulation on the particle mass and number emissions of two gasoline direct injection vehicles. Environ. Sci. Technol. 47, 11890–11896. https://doi.org/10.1021/es402686z.
McDonald, B.C., Goldstein, A.H., Harley, R.A., 2015. Long-term trends in California mobile source emissions and ambient concentrations of black carbon and organic aerosol. Environ. Sci. Technol. 49, 5178–5188. https://doi.org/10.1021/es505912b.
Ministry of Environmental Protection of the People's Republic of China (MEPPRC), 2017. China Vehicle Environmental Management Annual Report.
Miracolo, M.A., Drozd, G.T., Jathar, S.H., Presto, A.A., Lipsky, E.M., Corporan, E., Robinson, A.L., 2012. Fuel composition and secondary organic aerosol formation: gas-turbine exhaust and alternative aviation fuels. Environ. Sci. Technol. 46, 8493–8501. https://doi.org/10.1021/es300350c.
Nakao, S., Shrivastava, M., Nguyen, A., Jung, H., Cocker, D., 2011. Interpretation of secondary organic aerosol formation from diesel exhaust photooxidation in an environmental chamber. Aerosol Sci. Technol. 45, 964–972. https://doi.org/10.1080/02786826.2011.573510.
Ng, N.L., Kroll, J.H., Chan, A.W.H., Chhabra, P.S., Flagan, R.C., Seinfeld, J.H., 2007. Secondary organic aerosol formation from m-xylene, toluene, and benzene. Atmos. Chem. Phys. 7, 3909–3922. https://doi.org/10.5194/acp-7-3909-2007.
Odum, J.R., Jungkamp, T.P.W., Griffin, R.J., Forstner, H.J.L., Flagan, R.C., Seinfeld, J.H., 1997. Aromatics, reformulated gasoline, and atmospheric organic aerosol formation. Environ. Sci. Technol. 31, 1890–1897. https://doi.org/10.1021/es960535l.
Parrish, D.D., Zhu, T., 2009. Clean air for megacities. Science 326, 674–675. https://doi.org/10.1126/science.1176064.
Phuleria, H.C., Geller, M.D., Fine, P.M., Sioutas, C., 2006. Size-resolved emissions of organic tracers from light-and heavy-duty vehicles measured in a California roadway tunnel. Environ. Sci. Technol. 40, 4109–4118. https://doi.org/10.1021/es052186d.
Pirjola, L., Dittrich, A., Niemi, J.V., Saarikoski, S., Timonen, H., Kuuluvainen, H., Jarvinen, A., Kousa, A., Ronkko, T., Hillamo, R., 2016. Physical and chemical characterization of real-world particle number and mass emissions from city buses in Finland. Environ Sci Technol 50, 294–304. https://doi.org/10.1021/acs.est.5b04105.
Pope, C.A., Ezzati, M., Dockery, D.W., 2009. Fine-particulate air pollution and life expectancy in the United States. N. Engl. J. Med. 360, 376–386. https://doi.org/10.1056/NEJMsa0805646.
Presto, A.A., Gordon, T.D., Robinson, A.L., 2014. Primary to secondary organic aerosol: evolution of organic emissions from mobile combustion sources. Atmos. Chem. Phys. 14, 5015–5036. https://doi.org/10.5194/acp-14-5015-2014.
Reff, A., Bhave, P.V., Simon, H., Pace, T.G., Pouliot, G.A., Mobley, J.D., Houyoux, M., 2009. Emissions inventory of $PM_{2.5}$ trace elements across the United States. Environ. Sci. Technol. 43, 5790–5796. https://doi.org/10.1021/es802930x.
Robinson, A.L., Donahue, N.M., Shrivastava, M.K., Weitkamp, E.A., Sage, A.M., Grieshop, A.P., Lane, T.E., Pierce, J.R., Pandis, S.N., 2007. Rethinking organic aerosols: semivolatile emissions and photochemical aging. Science 315, 1259–1262. https://doi.org/10.1126/science.1133061.
Rönkkö, T., Virtanen, A., Kannosto, J., Keskinen, J., Lappi, M., Pirjola, L., 2007. Nucleation mode particles with a nonvolatile core in the exhaust of a heavy duty diesel vehicle. Environ. Sci. Technol. 41, 6384–6389. https://doi.org/10.1021/es0705339.
Rönkkö, T., Lähde, T., Heikkilä, J., Pirjola, L., Bauschke, U., Arnold, F., Schlager, H., Rothe, D., Yli-Ojanperä, J., Keskinen, J., 2013. Effects of gaseous sulphuric acid on diesel exhaust nanoparticle formation and characteristics. Environ. Sci. Technol. 47, 11882–11889. https://doi.org/10.1021/es402354y.
Sakurai, H., Park, K., McMurry, P.H., Zarling, D.D., Kittelson, D.B., Ziemann, P.J., 2003. Size-dependent mixing characteristics of volatile and nonvolatile components in diesel exhaust aerosols. Environ. Sci. Technol. 37, 5487–5495. https://doi.org/10.1021/es034362t.
Samy, S., Zielinska, B., 2010. Secondary organic aerosol production from modern diesel engine emissions. Atmos. Chem. Phys. 10, 609–625. https://doi.org/10.5194/acp-10-609-2010.
Schauer, J.J., Kleeman, M.J., Cass, G.R., Simoneit, B.R.T., 1999. Measurement of Emissions from Air Pollution Sources. 2. C1 through C30 Organic Compounds from Medium Duty Diesel Trucks. Environ. Sci. Technol. 33, 1578–1587. https://doi.org/10.1021/es980081n.
Shah, S.D., Cocker, D.R., Miller, J.W., Norbeck, J.M., 2004. Emission rates of particulate matter and elemental and organic carbon from in-use diesel engines. Environ. Sci. Technol. 38, 2544–2550. https://doi.org/10.1021/es0350583.
Shakya, K.M., Griffin, R.J., 2010. Secondary organic aerosol from photooxidation of polycyclic aromatic hydrocarbons. Environ. Sci. Technol. 44, 8134–8139. https://doi.org/10.1021/es1019417.
Tkacik, D.S., Lambe, A.T., Jathar, S., Li, X., Presto, A.A., Zhao, Y., Blake, D., Meinardi, S., Jayne, J.T., Croteau, P.L., Robinson, A.L., 2014. Secondary organic aerosol formation from in-use motor vehicle emissions using a potential aerosol mass reactor. Environ. Sci. Technol. 48, 11235–11242. https://doi.org/10.1021/es502239v.
Wang, X., Liu, T., Bernard, F., Ding, X., Wen, S., Zhang, Y., Zhang, Z., He, Q., Lu, S., Chen, J., Saunders, S., Yu, J., 2014a. Design and characterization of a smog chamber for studying gas-phase chemical mechanisms and aerosol formation. Atmos. Meas. Tech. 7, 301–313. https://doi.org/10.5194/amt-7-301-2014.
Wang, Y., Wang, M., Zhang, R., Ghan, S.J., Lin, Y., Hu, J., Pan, B., Levy, M., Jiang, J.H., Molina, M.J., 2014b. Assessing the effects of anthropogenic aerosols on Pacific storm track using a multiscale global climate model. Proc. Natl. Acad. Sci. U. S. A. 111, 6894–6899. https://doi.org/10.1073/pnas.1403364111.
Weitkamp, E.A., Sage, A.M., Pierce, J.R., Donahue, N.M., Robinson, A.L., 2007. Organic aerosol formation from photochemical oxidation of diesel exhaust in a smog chamber. Environ. Sci. Technol. 41, 6969–6975. https://doi.org/10.1021/es070193r.
Yao, Z., Shen, X., Ye, Y., Cao, X., Jiang, X., Zhang, Y., He, K., 2015. On-road emission characteristics of VOCs from diesel trucks in Beijing, China. Atmos. Environ. 103, 87–93. https://doi.org/10.1016/j.atmosenv.2014.12.028.
Ye, P.L., Ding, X., Hakala, J., Hofbauer, V., Robinson, E.S., Donahue, N.M., 2016. Vapor wall loss of semi-volatile organic compounds in a Teflon chamber. Aerosol Sci. Technol. 50, 822–834. https://doi.org/10.1080/02786826.2016.1195905.
Yeh, G.K., Ziemann, P.J., 2014. Alkyl nitrate formation from the reactions of C8–C14 n-alkanes with OH radicals in the presence of NOx: measured yields with essential corrections for gas–wall partitioning. J. Phys. Chem. A 118, 8147–8157. https://doi.org/10.1021/jp500631v.
Yi, Z., Wang, X., Sheng, G., Zhang, D., Zhou, G., Fu, J., 2007. Soil uptake of carbonyl sulfide in subtropical forests with different successional stages in south China. J. Geophys. Res.-Atmos. 112. https://doi.org/10.1029/2006jd008048.
Zavala, M., Molina, L.T., Yacovitch, T.I., Fortner, E.C., Roscioli, J.R., Floerchinger, C., Herndon, S.C., Kolb, C.E., Knighton, W.B., Paramo, V.H., Zirath, S., Mejía, J.A.,

Jazcilevich, 2015. Emission factors of black carbon and co-pollutants from diesel vehicles in Mexico City. Atmos. Chem. Phys. 17, 15293–15305. https://doi.org/10.5194/acp-17-15293-2017.

Zhang, Q., Streets, D.G., Carmichael, G.R., He, K.B., Huo, H., Kannari, A., Klimont, Z., Park, I.S., Reddy, S., Fu, J.S., Chen, D., Duan, L., Lei, Y., Wang, L.T., Yao, Z.L., 2009. Asian emissions in 2006 for the NASA INTEX-B mission. Atmos. Chem. Phys. 9, 5131–5153. https://doi.org/10.5194/acp-9-5131-2009.

Zhang, X., Cappa, C.D., Jathar, S.H., McVay, R.C., Ensberg, J.J., Kleeman, M.J., Seinfeld, J.H., 2014. Influence of vapor wall loss in laboratory chambers on yields of secondary organic aerosol. Proc. Natl. Acad. Sci. U. S. A. 111, 5802–5807. https://doi.org/10.1073/pnas.1404727111.

Zhang, X., Schwantes, R.H., McVay, R.C., Lignell, H., Coggon, M.M., Flagan, R.C., Seinfeld, J.H., 2015. Vapor wall deposition in Teflon chambers. Atmos. Chem. Phys. 15, 4197–4214. https://doi.org/10.5194/acp-15-4197-2015.

Zhang, Y., Wang, X., Wen, S., Herrmann, H., Yang, W., Huang, X., Zhang, Z., Huang, Z., He, Q., George, C., 2016. On-road vehicle emissions of glyoxal and methylglyoxal from tunnel tests in urban Guangzhou, China. Atmos. Environ. 127, 55–60. https://doi.org/10.1016/j.atmosenv.2015.12.017.

Zhao, Y., Nguyen, N.T., Presto, A.A., Hennigan, C.J., May, A.A., Robinson, A.L., 2015. Intermediate volatility organic compound emissions from on-road diesel vehicles: chemical composition, emission factors, and estimated secondary organic aerosol production. Environ. Sci. Technol. 49, 11516–11526. https://doi.org/10.1021/acs.est.5b02841.

Zhao, Y., Saleh, R., Saliba, G., Presto, A.A., Gordon, T.D., Drozd, G.T., Goldstein, A.H., Donahue, N.M., Robinson, A.L., 2017. Reducing secondary organic aerosol formation from gasoline vehicle exhaust. Proc. Natl. Acad. Sci. USA 114, 6984–6989. https://doi.org/10.1073/pnas.1620911114.

Zheng, X., Wu, Y., Jiang, J., Zhang, S., Liu, H., Song, S., Li, Z., Fan, X., Fu, L., Hao, J., 2015. Characteristics of on-road diesel vehicles: black carbon emissions in Chinese cities based on portable emissions measurement. Environ. Sci. Technol. 49, 13492–13500. https://doi.org/10.1021/acs.est.5b04129.